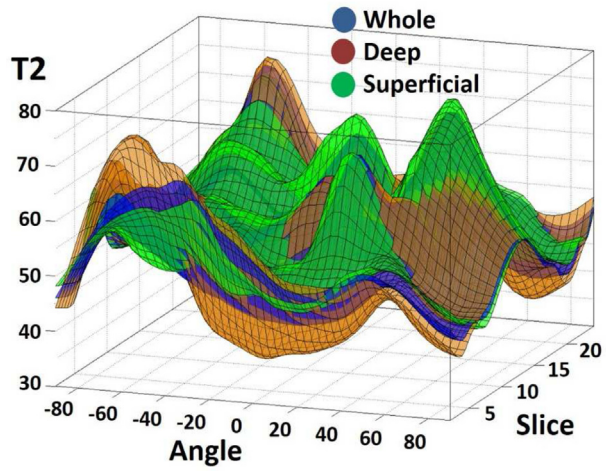

Figure 3. 3D graph of the entire femoral cartilage.

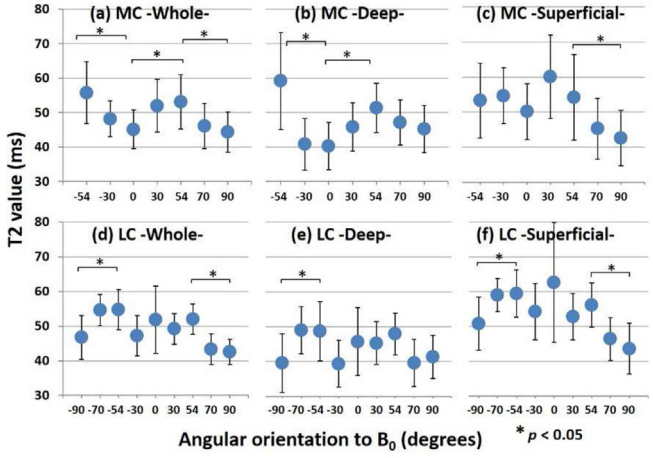

Figure 4. Comparison of T2 values between magic angle and others.

362

COMPARISON OF T1RHO IMAGING BETWEEN SPOILED GRADIENT ECHO (SPGR) AND BALANCED STEADY STATE FREE PRECESSION (B-FFE) SEQUENCE OF KNEE CARTILAGE AT 3 TESLA MRI

T. Nozaki, Y. Kaneko, H. Yu, K. Kaneshiro, R. Schwarzkopf, H. Yoshioka.
Univ. of California Irvine, Orange, CA, USA

Purpose: T1rho-weighted MR imaging has recently been proposed as an attractive biomarker to existing conventional morphological MRI methods, and has been shown to be more sensitive to biochemical change in cartilage than T2 mapping. It enables us to detect early cartilage degeneration in early osteoarthritis patients before appearing morphological change. However the factors affecting the T1rho mapping such as MR sequences and operator-dependent manual cartilage segmentation is not well understood. Regarding MRI sequences, there are two basic types of fast gradient echo (GRE) sequences used in T1 rho mapping. One is a spoiled GRE sequence; residual transverse magnetization is spoiled. The other is a steady-state GRE sequence; transverse magnetization is not spoiled but is refocused to contribute to steady-state formation. The objective of this study was to investigate the difference of T1rho profiles between spoiled gradient echo (SPGR) and balanced steady state free precession (b-FFE) sequences.

Methods: 20 healthy volunteers (mean: 28.9 y.o., range: 19-38) were enrolled in this study. The study was approved by IRB, and written informed consent was obtained from each subject. T1rho images of the knee were acquired with two types of pulse sequence: b-FFE and SPGR. All MR studies were performed on a 3.0-T unit (Achieva, Philips Healthcare, Netherland) utilizing an 8-channel knee receive-only RF-coil. Two sagittal T1rho-weighted images of each subject were acquired on the pulse sequence of b-FFE and SPGR. The acquisition parameters were as follows. SPGR: mode = 3D, fat-saturation method = PROSET, TR/TE = 6.4/3.4msec, Band width = 475Hz, ETL = 64, NEX = 1, FOV = 140*140mm, Slice thickness/gap = 3/0mm, Flip angle = 10 degree, Image-matrix = 512*512mm, number of slices = 31, Time of spin-lock (TSL) = 20/40/60/80msec, acquisition time = 4min09sec *4, b-FFE: mode = 3D, fat-saturation method = SPIR, TR/TE = 4.8/2.4msec, Band width = 606 Hz, ETL = 154, NEX = 1, FOV = 140*140mm, Slice thickness/gap = 3/0mm, Flip angle = 25 degree, Image-matrix = 512*512mm, number of slices = 31, Time of spin-lock (TSL) = 20/40/60/80msec, acquisition time = 3min57sec *4 Entire knee cartilage segmentation was performed by two raters independently slice by slice with Matlab (Fig.1). Inter- and intra- observer reproducibility between two imaging protocols was calculated. Relative signal intensity (SI) of each structure and relative contrast between structures of the knee were also quantitatively measured using Mann-Whitney test. The difference of T1rho values between SPGR and b-FFE sequences was statistically analyzed using the Wilcoxon signed-rank test.

Results: Average T1rho value of the entire knee cartilage on b-FFE was higher than on SPGR with significant difference ($p<0.05$) (Fig.2). The reproducibility of the segmented area and T1rho values was superior on SPGR than b-FFE (Table1). The intraclass correlation coefficient was 0.878 on SPGR and 0.836 on b-FFE, and the interclass correlation coefficient was 0.846 on SPGR and 0.824 on b-FFE, regarding to T1rho values. The relative SI of fluid was higher on SPGR, while that of subchondral bone was higher on b-FFE with significant difference ($p<0.001$) (Fig.3). There were also significant differences in relative fluid-cartilage, fluid-subchondral bone, and cartilage-subchondral bone contrast ($p<0.001$, respectively) between two sequences (Fig.4). These results suggest that the outline between subchondral bone and cartilage is more distinct on SPGR, although there is a possibility that negative contrast between fluid and cartilage better delineate cartilage surface on b-FFE.

Conclusions: Inter-reader and intra-reader reproducibility of measurement on knee cartilage T1rho mapping are excellent on both sequences and higher on SPGR than b-FFE. T1rho value tends to be higher on b-FFE than SPGR. We need to pay attention to factors of different sequences which causes variability of T1rho value in clinical applications.

Table 1
ICCs and B-A plots for intraobserver and interobserver reproducibility.

		Analyses	SPGR	b-FFE
Interobserver reproducibility	T1rho value	Interclass correlation coefficient	0.846 (0.757, 0.904)	0.824 (0.665, 0.903)
	Segmented pixels	BA-correlation plot; r-value	0.641	0.588
		BA-difference plot; r-value	-0.065	-0.036
Intraobserver reproducibility	T1rho value	Intraclass correlation coefficient	0.878 (0.806, 0.925)	0.836 (0.741, 0.898)
	Segmented pixels	BA-correlation plot; r-value	0.858	0.796
		BA-difference plot; r-value	0.171	0.160

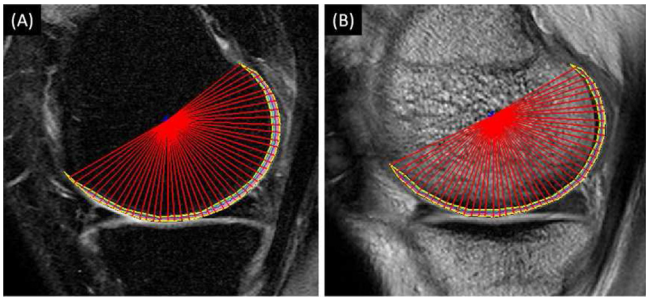

Figure 1. Sagittal images from T1rho sequence of knee MRI after manual segmentation with post-processing. (A) SPGR (B) b-FFE.

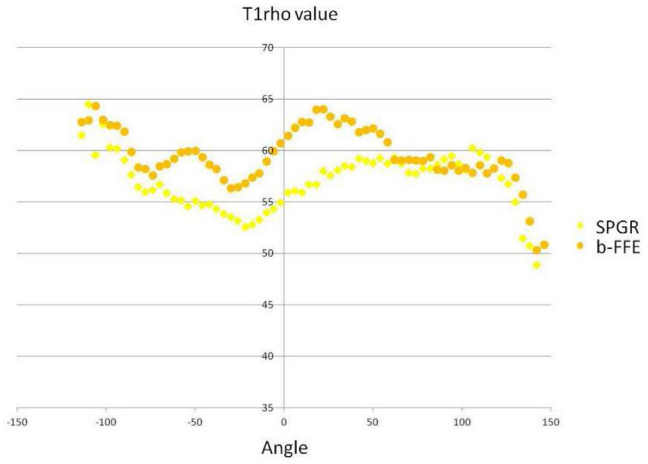

Figure 2. Comparison of T1rho value of entire knee cartilage between SPGR and b-FFE.

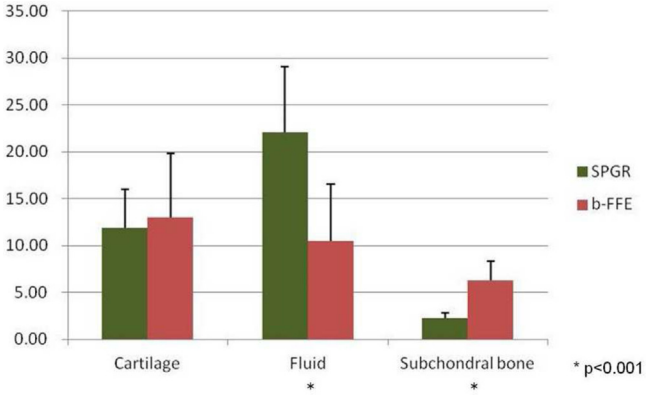

Figure 3. Mean values of relative signal intensity.

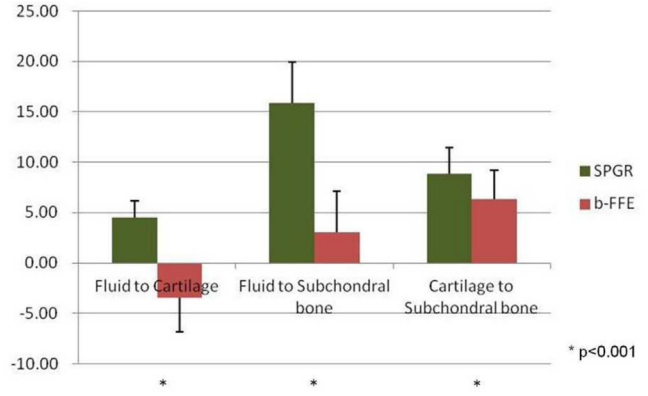

Figure 4. Mean values of relative contrast.

363

TEST-RETEST RELIABILITY OF TIBIOFEMORAL JOINT SPACE WIDTH MEASUREMENTS USING LOW-DOSE STANDING CT

N.A. Segal †, J. Bergin ‡, C. Findlay ‡, D.D. Anderson ‡. † *Univ. of Kansas, Kansas City, KS, USA;* ‡ *Univ. of Iowa, Iowa City, IA, USA*

Purpose: Tibiofemoral joint space width (JSW), measured from plain radiographs, is the only structural outcome currently approved by the FDA for evaluating knee OA progression in clinical trials. While inexpensive and readily available, overlapping bony structures on 2D images make JSW measured from plain radiographs insensitive. This measure fails to detect changes in JSW for years after OA begins and requires > 3 years to detect progression. 3D images acquired using a low-dose standing CT (SCT) scanner are unencumbered by overlapping anatomy and may allow for more reliable JSW measurement, which would improve the monitoring of disease and speed the pace of scientific discovery. If found to be reliable, the proposed imaging procedure may become an attractive replacement for weight-bearing knee radiographs. Thus, our objective was to evaluate the test-retest reliability of SCT measurements of JSW.

Methods: Twenty-seven men and women, age 40 and older, with known KL grade 0-3 knees, chosen to represent a range of knee OA features, were recruited from the University of Iowa Hospitals and Clinics. Bilateral approximately 20° fixed-flexed SCT images of the tibiofemoral joint were acquired at visits two weeks apart. Tibial and femoral bone surfaces were extracted from the CT images using a semi-automated watershed transform-based algorithm implemented in MATLAB (The Mathworks, Natick, MA). A 3D triangulated surface mesh for each bone was generated and lightly smoothed to reduce voxellation artifact. Tibiofemoral JSW was quantified using a nearest-neighbor algorithm implemented in MATLAB. For each compartment, we defined the area for evaluation as that with a JSW < 10mm. The fractions of this area with JSW below thresholds between 2 and 5mm were calculated. JSW distributions for a representative knee scanned at baseline and 2 weeks later are depicted in the accompanying Figure. Test-retest reliability of the JSW measurements were assessed using Intraclass Correlation Coefficients (ICC 2,1) for the fractions below each threshold, using the Shrout-Fleiss fixed set method.

Results: Participants were 65.4% female (mean±SD age 58.2±11.3 years; BMI 29.1±5.6 kg/m^2). Four knees could not be segmented due to either lack of follow-up or movement during the scan on at least one visit. Therefore, 50 knees were included: 14 KL0, 5 KL1, 12 KL2 and 19 KL3 on

Test-Retest Reliability of 3D JSW By SCT

% Joint Area Below JSW (mm)	Lateral Compartment		Medial Compartment	
	ICC	ICC 95%CI	ICC	ICC 95%CI
5.0	0.97	0.94, 0.98	0.94	0.90, 0.97
4.5	0.97	0.94, 0.98	0.94	0.90, 0.96
4.0	0.95	0.92, 0.97	0.96	0.92, 0.97
3.5	0.95	0.91, 0.97	0.97	0.94, 0.98
3.0	0.97	0.94, 0.98	0.96	0.94, 0.98
2.5	0.97	0.94, 0.98	0.90	0.84, 0.94
2.0	0.97	0.95, 0.98	0.91	0.85, 0.95